Theor Appl Climatol (2012) 109:233–243
DOI 10.1007/s00704-011-0576-8

ORIGINAL PAPER

Ensemble empirical mode decomposition for tree-ring climate reconstructions

Feng Shi · Bao Yang · L. von Gunten · Chun Qin · Zhangyong Wang

Received: 2 September 2011 / Accepted: 14 December 2011 / Published online: 30 December 2011

Abstract A novel data adaptive method named ensemble empirical mode decomposition (EEMD) was used to reconstruct past temperature and precipitation variability in two 2,328- and 1,837-year tree-ring chronologies from the Dulan region, northeastern Qinghai–Tibetan Plateau. Our results show that EEMD can be used to extract low-frequency signals from the Dulan tree-ring data. The extracted low-frequency temperature trends in the two chronologies correlate significantly with Northern Hemisphere temperatures over the past two millennia. In addition, the newly reconstructed precipitation data have a higher standard deviation than that of data reconstructed with the conventional ordinary least squares and variance matching methods and yield the best amplitude match to the instrumental data. This study shows that EEMD is a powerful tool for extracting the full spectrum of climate information in tree-ring chronologies.

1 Introduction

A major problem in modern dendroclimatology is that the methods traditionally used for tree-ring climate reconstructions are not well suited to reconstructing the low-frequency signals of climatic variability (Moberg et al. 2005; Esper et al. 2002). The traditional process of tree-ring climate reconstruction includes two main steps. Firstly, a chronology is established using the measured tree-ring widths. Briffa et al. (1992, 2008) have applied a regional curve standardization approach to improve the preservation of low frequency variances. This method was further improved by Yang et al. (2012a, b) who introduced an eigenvalue analysis technique and by Melvin and Briffa (2008) who used a signal-free approach to effectively exclude the effects of tree age and microenvironments in their tree-ring chronologies. The second step is the calibration/verification process based on established chronologies. The conventional methods include the simple ordinary least squares (OLS) and variance matching (VM) methods. Moberg et al. (2005) have tried to extract low-frequency climate information from various proxy-type data using wavelet analysis to establish a regression equation. The drawback of these "conventional" methods is that, in theory, they can only be applied to linear and stationary data, whereas long-term climate variability is usually characterized by non-linear and non-stationary behavior (Lee and Ouarda 2011).

Recognizing this problem, Huang et al. (1998) proposed a new method to handle nonlinear and non-stationary time series called empirical mode decomposition (EMD). Later, Wu et al. (2009) further developed the EMD model to resolve the EMD mode-mixing problem, leading to the ensemble empirical mode decomposition (EEMD) model. In this study, we test the suitability of the EEMD method for reconstructing past temperatures and precipitation in two tree-ring series from the Dulan region on the northeastern Qinghai–Tibetan Plateau.

Due to its high topography, the Qinghai–Tibetan Plateau strongly affects the large-scale atmospheric circulation over Asia and is thus an important region for climate change

Electronic supplementary material The online version of this article (doi:10.1007/s00704-011-0576-8) contains supplementary material, which is available to authorized users.

F. Shi · B. Yang (✉) · C. Qin · Z. Wang
Key Laboratory of Desert and Desertification, Cold and Arid Regions Environmental and Engineering Research Institute, Chinese Academy of Sciences,
320 Donggang West Road,
730000, Lanzhou, China
e-mail: yangbao@lzb.ac.cn

L. von Gunten
Institute of Geography and Oeschger Centre for Climate Change Research, University of Bern,
Bern, Switzerland

research in East Asia (Liu and Chen 2000; Webster and Tomas 1998; Yang et al. 2010). The natural climate archives on the Qinghai–Tibetan Plateau are very sensitive to past climate changes (Feng et al. 1998). Furthermore, the oldest trees in China, Qilian junipers (*Juniperus przewalskii* Kom, better known in China as *Sabina przewalskii*), can be found on the eastern part of the Tibetan Plateau. Of particular interest for dendrochronological research, archaeological wood is widespread in the region, allowing for the creation of millennial-scale time series. Therefore, the Qinghai–Tibetan Plateau has been an important region for dendroclimatological research for many years (Sheppard et al. 2004; Zhang et al. 2003; Liu et al. 2009, 2006; Zhu et al. 2008; Shao et al. 2009; Shao et al. 2005; Zhang and Qiu 2007; Liu et al. 2005; Gou et al. 2006; Zhang et al. 2009; Trenberth 1984). The first tree-ring chronology in the Dulan region was a 1,835-year series developed by Kang et al. (1997). Since then, many other scholars have created tree-ring chronologies and climate reconstructions for the Dulan region (Liu et al. 2009, 2006; Zhang et al. 2003). However, despite the large number of high-quality tree-ring records available from the region, to date, only few attempts have been made to extract the low-frequency climate signals from those series (e.g., Yang et al. 2012a, b).

Here, two Dulan tree-ring width chronologies as well as instrumental temperature and precipitation data are decomposed by the EEMD method in different time frequency domains. The low-frequency climate signals from the Dulan tree-ring width chronologies are extracted by the EEMD method and the climatic significance of the chronologies is assessed.

2 Data and methods

2.1 Instrumental data

Dulan (ca. 35°50′ N–36°30′ N, 97°40′ E–98°20′ E) is located on the northeastern Qinghai–Tibetan Plateau (Fig. 1). The region is characterized by a continental arid climate and is primarily influenced by the prevailing Westerlies. However, because the region is located very closely to the present northwestern boundary of the Asian summer monsoon, it is likely to be sensitive to variations in the strength of both of these atmospheric circulation patterns (Yang et al. 2011). The China Meteorological Data Sharing Service System provided daily instrumental data from the Dulan meteorological station (36°03′ N, 98°01′ E, 3,192 m a.s.l., continuous data from 16 January 1954 to 30 June 2010). In this study, we define the daily average temperature as the arithmetic average of the daily maximum and minimum temperatures to ensure homogeneity (Li et al. 2010; Tang et al. 2009; Brohan et al. 2006). Mean annual total precipitation in this area was 199.5 mm for the period AD 1955–2009, with 97% of the annual rainfall occurring between May and September (Fig. 2). Mean annual air temperature was 3.8°C during the same period.

2.2 Climatic proxy data

There are two available versions of the Dulan chronologies, established by Zhang et al. (2003) and Sheppard et al. (2004) (hereafter referred to as "Z03" and "S04"). Both chronologies were revised by Shao et al. (2009), who found two missing rings in the two series. Z03 combines living trees and archaeological wood and covers 2,328 years; S04 only uses living trees and covers 1,837 years. The Pearson correlation coefficient of the two undecomposed chronologies over the overlapping period AD 157 to 1993 is $r=0.86$ ($p<10^{-5}$).

Correlation analyses with meteorological data were carried out between the annual tree-ring chronologies and the annual precipitation from July of the previous year to June of the current year and between the annual tree-ring chronologies and the mean temperatures of the preceding year (Liu et al. 2009, 2006; Zhang et al. 2003). The correlation coefficients for S04 from AD 1955–1993 are 0.68 ($p<10^{-5}$) for precipitation and 0.22 ($p>0.1$) for temperature. Those for Z03 from 1955–2000 are 0.67 ($p<10^{-5}$) and 0.13 ($p>0.1$), respectively. The highly significant correlations with precipitation indicate that the two standard (STD, i.e., not decomposed by EEMD) chronologies can be used to reconstruct past precipitation. There is also a weak positive, but non-significant, correlation with the average temperature of the previous year. In this paper, we use these statistical relationships to reconstruct mean annual precipitation from previous July to current June and the previous year's temperature.

2.3 Statistical methods

The EMD was designed specifically for analyzing nonlinear and non-stationary data. Therefore, it is well suited to long tree-ring time series. EMD can be used to decompose any data set into a finite and often small number of monocomponent signals, called intrinsic mode functions (IMFs, e.g., Wu et al. 2011). The frequencies of the IMFs help in identifying the nested structure of a data set and take full account of the nonlinear characteristics of the original data (Huang and Wu 2008; Huang et al. 1998). To overcome the scale-mixing problem, a new noise-assisted data analysis method was proposed: the EEMD (Wu et al. 2009, 2008). The first step of this method provides a relatively consistent reference size distribution by adding a white noise series to the target data. In the second step, the data with white noise is decomposed into IMFs. After several iterations of steps 1 and 2, the cumulative effect of the added white noise is reduced to a negligible level, and finally the ensemble

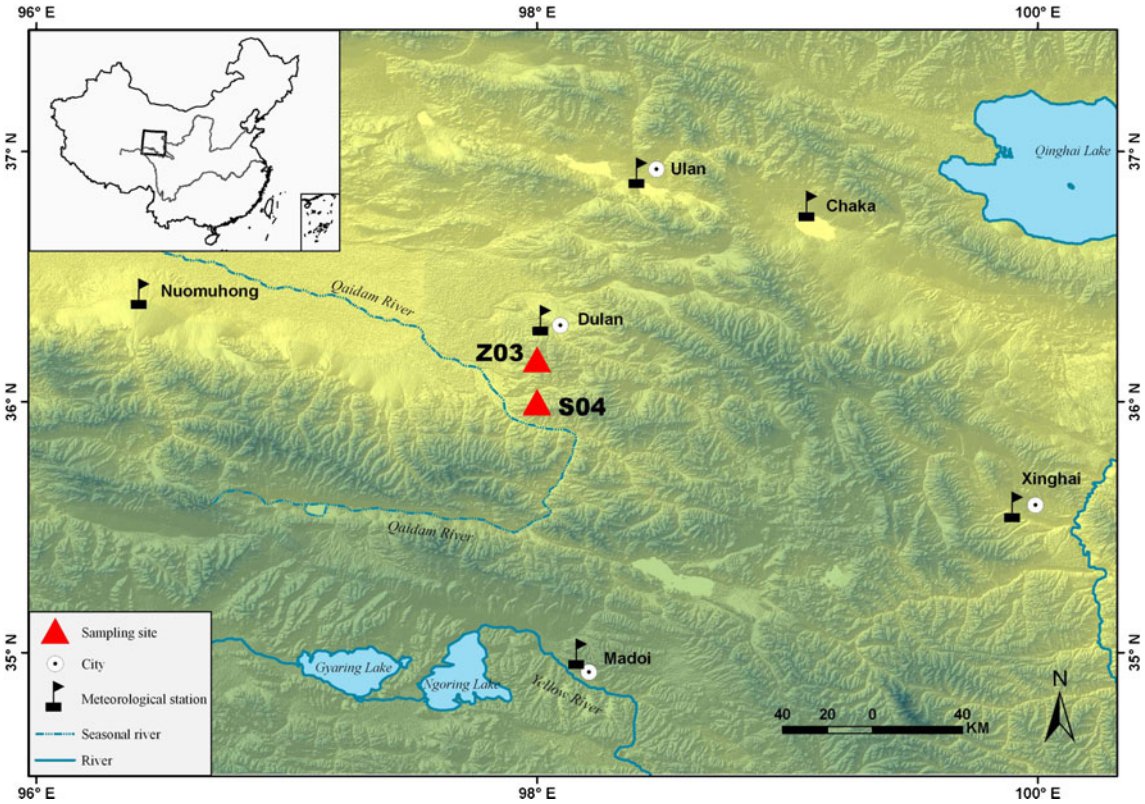

Fig. 1 Map of the tree-ring sampling sites and neighboring meteorological stations

means of corresponding IMFs of the decompositions with the same time scales are obtained.

Traditionally, instrumental data anomalies from several climate stations are defined as the departure of a climate parameter from its mean during a particular period (e.g., AD 1961–1990 for annual mean data anomalies) and represent the climate variability at various time scales (Glickman and Zenk 2000). However, this method does not effectively account for the intrinsic nonlinearity of the climate system (Wu et al. 2008). Therefore, Wu et al. (2008) proposed a new anomaly reference frame named the modulated annual cycle (MAC), which uses the amplitude of annual cycles from year to year instead of a constant value (Qian et al. 2010; Wu et al. 2008; Huang and Wu 2008). Here, we use the MAC anomaly reference frame to effectively extract seasonal and annual cycles from the meteorological data

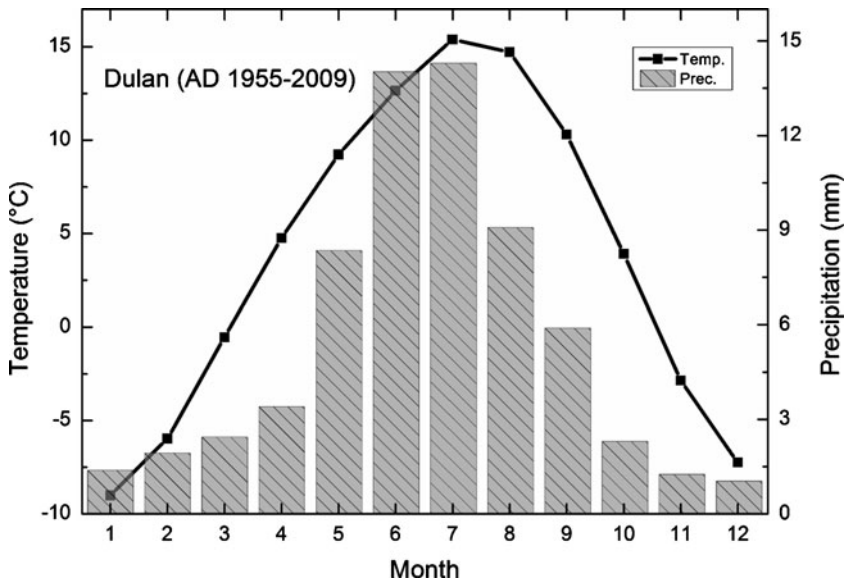

Fig. 2 Climate diagram for Dulan, northeastern Qinghai–Tibetan Plateau, during the period 1955–2009

series. Note that the prerequisite for the use of the EEMD method is that the considered tree-ring chronology is strongly correlated to meteorological data in the calibration period. The itemized steps are as follows:

Step 1. processing of instrumental data

We first decomposed the daily instrumental data (including the precipitation and temperature data) using the EEMD method. We stopped the EEMD calculations after 1,000 iterations since further iteration steps did not improve the results significantly. A total of 14 IMFs for precipitation and temperature data were detected. We excluded the sub-annual IMFs before extracting seasonal and annual cycle signals from the meteorological data series.

Step 2. processing of proxy data

We decomposed the two tree-ring chronologies (Z03 and S04) using the EEMD method, again stopping calculations after 1,000 iterations. The EEMD decomposed the S04 chronology into 10 IMFs and the Z03 chronology into 11 IMFs. Then, we applied a wavelet analysis (Torrence and Compo 1998) for every IMF of the tree-ring chronology S04 to determine the number of cycles per IMF.

Step 3. regression of proxy data

We used the EEMD components of the two tree-ring chronologies to reconstruct the past climate change using the "variance matching method" (Lee et al. 2008; Jones et al. 1998) in different frequency bands. For S04, the calibration and validation periods were AD 1955–1984 and AD 1985–1993, respectively. We used the same calibration period for the Z03 chronology and a validation period of AD 1985–2000. Where necessary, the p values of the Pearson calibration were corrected for autocorrelation following Trenberth (1984). To compare the EEMD approach with the conventional regression methods, the simple OLS and VM methods were also used to calibrate the original (undecomposed) chronologies following Jones et al. (1998).

Step 4. validation of reconstruction

We used the "leave-one-out" cross-validation approach (Cook et al. 2010) to provide a goodness-of-fit measure. Reconstruction quality was measured by the correlation coefficient (r^2) between the observed and reconstructed temperatures during the verification period. Further reconstruction skills were measured by the reduction of error and the coefficient of efficiency statistics (Cook et al. 2010). We calculated the uncertainties of the reconstruction using the following equation (Mann et al. 2008):

$$uncert. = std \cdot \sqrt{1 - r^2} \quad (1)$$

where "uncert." is the uncertainty, "std" is the standard deviation of instrumental data during the calibration period, and r^2 is the squared correlation coefficient during the verification period. All statistical validation results for the reconstruction, skill assessment, and uncertainty estimation are shown in Table S4.

3 Results and discussion

The decomposed series of the two tree-ring chronologies and instrumental records from Dulan are shown in Table S1. The eighth IMF of the precipitation data and the sixth IMF

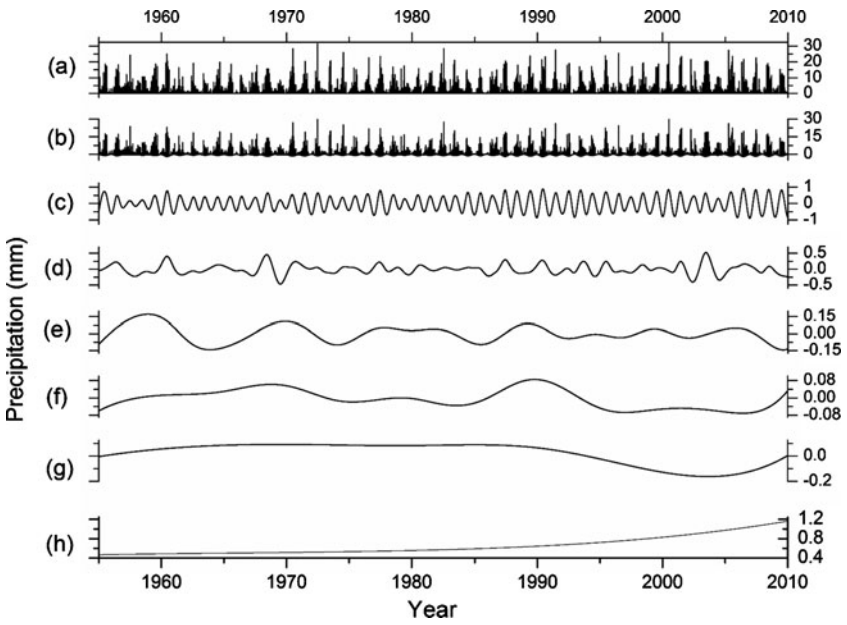

Fig. 3 **a** Daily precipitation (mm) instrumental record at the Dulan meteorological station during AD 1955–2010. The seven EEMD components are: **b** the high frequency component (1.5–4.0 years), **c** a modulated annual cycle component, **d** 2–4 year component, **e** 6.0–9.0 year component, **f** 10–16 year component, **g** 20–70 year component, and **h** trend component (>100 years)

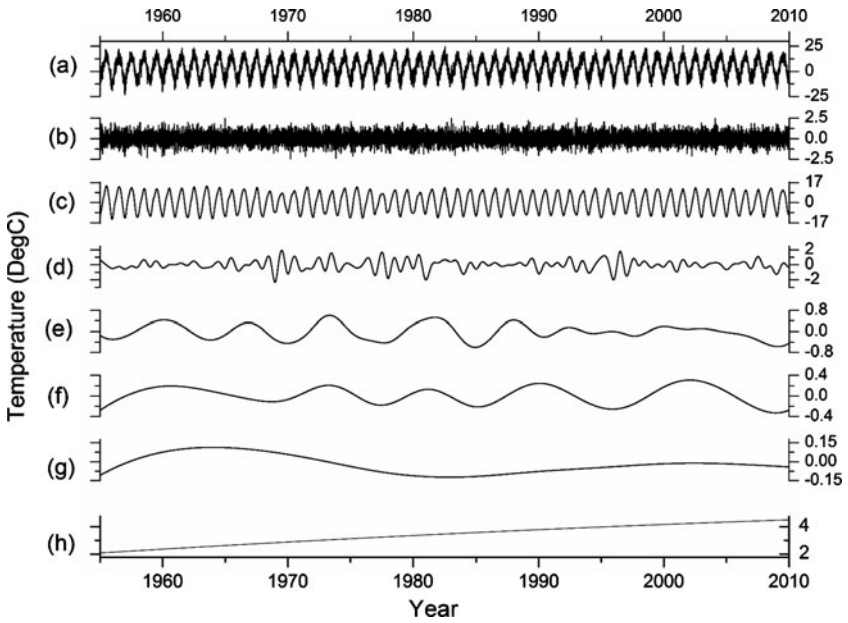

Fig. 4 **a** Daily surface air temperature measured at the Dulan meteorological station during AD 1955—2009 and its seven components obtained using the EEMD method: **b** the high frequency component (1.5–4.0 years), **c** a modulated annual cycle component, **d** 2–4 year component, **e** 6.0–9.0 year component, **f** 10–16 year component, **g** 20–70 year component, and **h** trend component (>100 years)

of the temperature records represent the annual cycle. According to the trend components (the final residual) of the instrumental records, the temperature and precipitation have monotonically increased since AD 1955.

The IMF analysis of the daily instrumental data shows that the EEMD method was well suited to extracting high-frequency signals with periods less than 20 years from the original data set. However, instrumental data in Dulan only cover the last 55 years; thus, it was not possible to extract lower-frequency (>20 years) signals. In the millennial-scale proxy data, it was possible to extract decadal and centennial signals.

The quasi-period of each component is shown in Table S2. Because of natural variability and non-linearity in the system, the IMFs of the meteorological and tree-ring data do not have exactly the same cycles. In order to decompose the tree-ring series, we therefore chose frequency bands covering the range of detected quasi-periods. The exact cycle frequencies of each analysis band were assessed in a later step using wavelet analysis.

The first IMF of the two tree-ring chronologies had a 3-year periodic oscillation. Similar components were detected in the meteorological temperature (ca. 3.2 years) and precipitation (ca. 3.5 years) data. However, temperature and precipitation IMFs also had components with periods of ca. 2.1 and 1.5 years; therefore, we set the first frequency analysis band to cover the range 1.5–4.0 years to include more inter-annual variability (panel b in Figs. 3, 4, 5, and 6). The second component of the two tree-ring chronologies was a ca. 6.5-years periodic oscillation. Similar components were detected in the temperature and precipitations data at around 7.6 and 8.7 years. Therefore, we set the second frequency band to cover 6.0–9.0 years (panel e in Figs. 3, 4, 5, and 6). Next, the third band was set to cover a frequency band of 10–16 years (panel f in Figs. 3, 4, 5, and 6), given the third IMFs of the two tree-ring series (ca. 13.3 and 14.2 year oscillations) and the

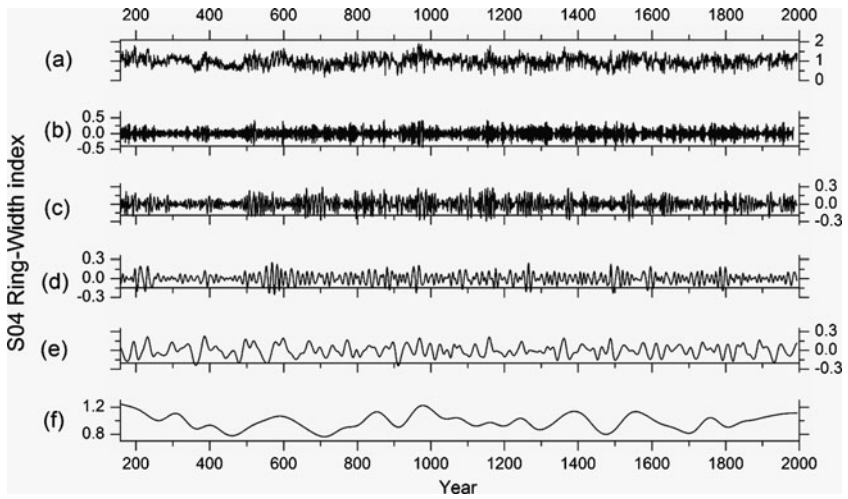

Fig. 5 **a** S04 tree-ring width index at Dulan for AD 157–1993 and its five components obtained using the EEMD method: **b** the high frequency component (1.5–4.0 years), **c** 6.0–9.0 year component, **d** 10–16 year component, **e** 20–70 year component, and **f** trend component (>100 years)

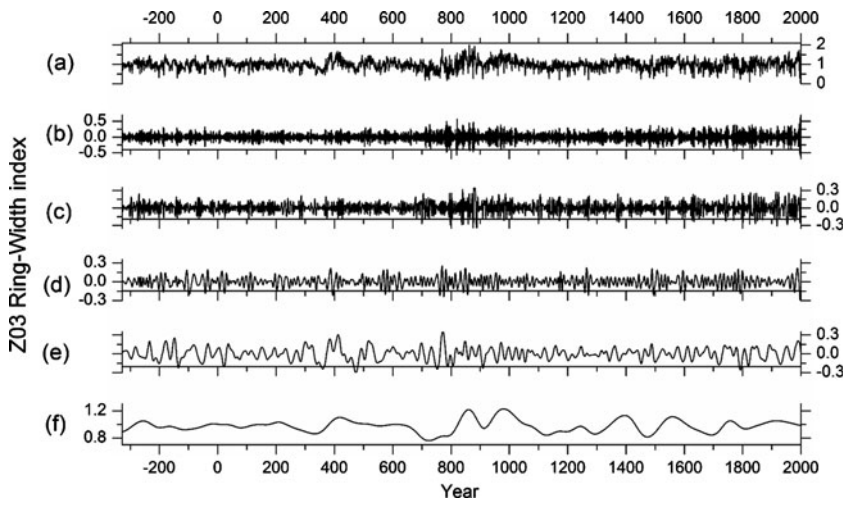

Fig. 6 **a** Z03 tree-ring width index at Dulan for 328 BC–AD 2000 and its five components obtained using the EEMD method: **b** the high frequency component (1.5–4.0 years), **c** 6.0–9.0 year component, **d** 10–16 year component, **e** 20–70 year component, and **f** trend component (>100 years)

10th and 12th IMFs of the temperature and precipitation data (ca. 10.3- and 16.2-year oscillations, respectively). The fourth frequency analysis band was set to 20–70 years (panel g in Figs. 3, 4, 5, and 6) because the 13th IMF of the precipitation data had a 37.8-year periodic oscillation, and the 11th to 13th IMFs of the temperature data had periodic oscillations with periods of >56.7 years, and the fourth and fifth IMFs of the two tree-ring chronologies had periodic oscillations of 27.9, 28.3, 65.6, and 69.3 years (Table S2). The remaining components were covered by the fifth frequency analysis band and represent the 100-year to trend component (panel h in Figs. 3, 4, 5, and 6).

Figures 3 and 4 illustrate that, except for the high-frequency signal, the annual cycle is the most prominent component in the meteorological temperature and precipitation data.

The wavelet analysis was used to detect cycles in the decomposed frequency components of the tree-ring series. Results from the wavelet analysis (Fig. 7) over the full reconstruction period (AD 157–1993) showed that there were several significant and stable periodic oscillations, plus the trend (fifth component) reflecting a non-stationary feature. The first, second, and third components of the S04 STD revealed cycles with periods of ca. 3.0, 6.5, and

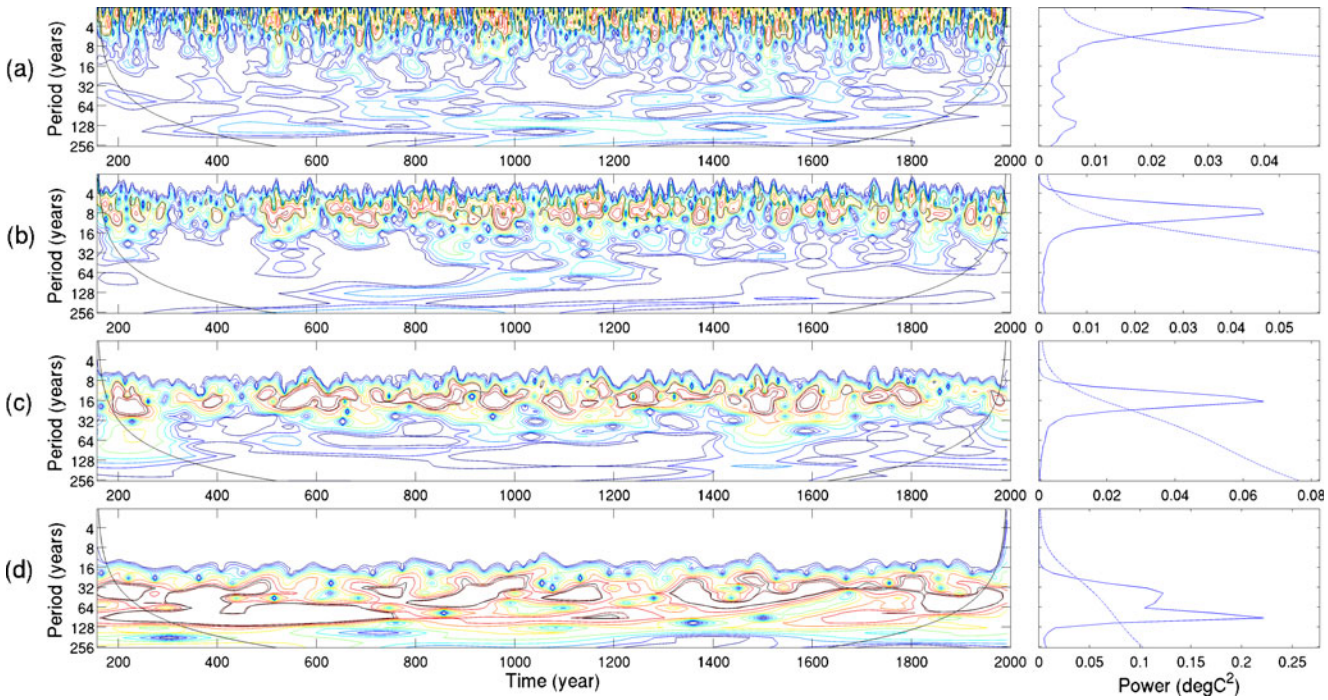

Fig. 7 Power spectra of the EEMD components in the S04 STD chronology: **a** first component, **b** second component, **c** third component, and **d** fourth component

13.3 years, respectively, while the fourth component showed two cycles, with periods of 28.3 and 69.3 years.

Table S3 shows the correlation analysis between the two tree-ring chronologies and meteorological data in the five time–frequency domains. The correlation coefficients between the two tree-ring chronologies over the period 157–1993 for the first four components all exceeded 0.77 ($p< 10^{-4}$), and the correlation coefficient of the trend term reached 0.67 ($p=0.33$). This indicates that the two chronologies were characterized by similar oscillation frequencies in all the time–frequency domains.

The correlation between the annual average temperature and precipitation data in the first four time–frequency domains was not significant, but the correlation coefficient of the last trend item was significant ($r=0.88$, $p=0.05$). This indicates that annual temperature and precipitation in Dulan follow the same trend at century or longer time scales and that the Dulan climate likely follows a "warm–wet" and "cold–dry" pattern over long time scales. The two STD chronologies were significantly correlated with the precipitation series (AD 1955–1993 and 1955–1999) in the first three time–frequency domains but were not significantly correlated with temperature. This indicates that the two chronologies do indeed provide a good proxy for high-frequency variations in annual precipitation. Thus, we have a reason to believe that the two chronologies will also respond to the lower-frequency characteristics of annual precipitation. Nevertheless, because of the short instrumental data time series, the tree-ring chronology cannot be properly matched in the low-frequency domain of the

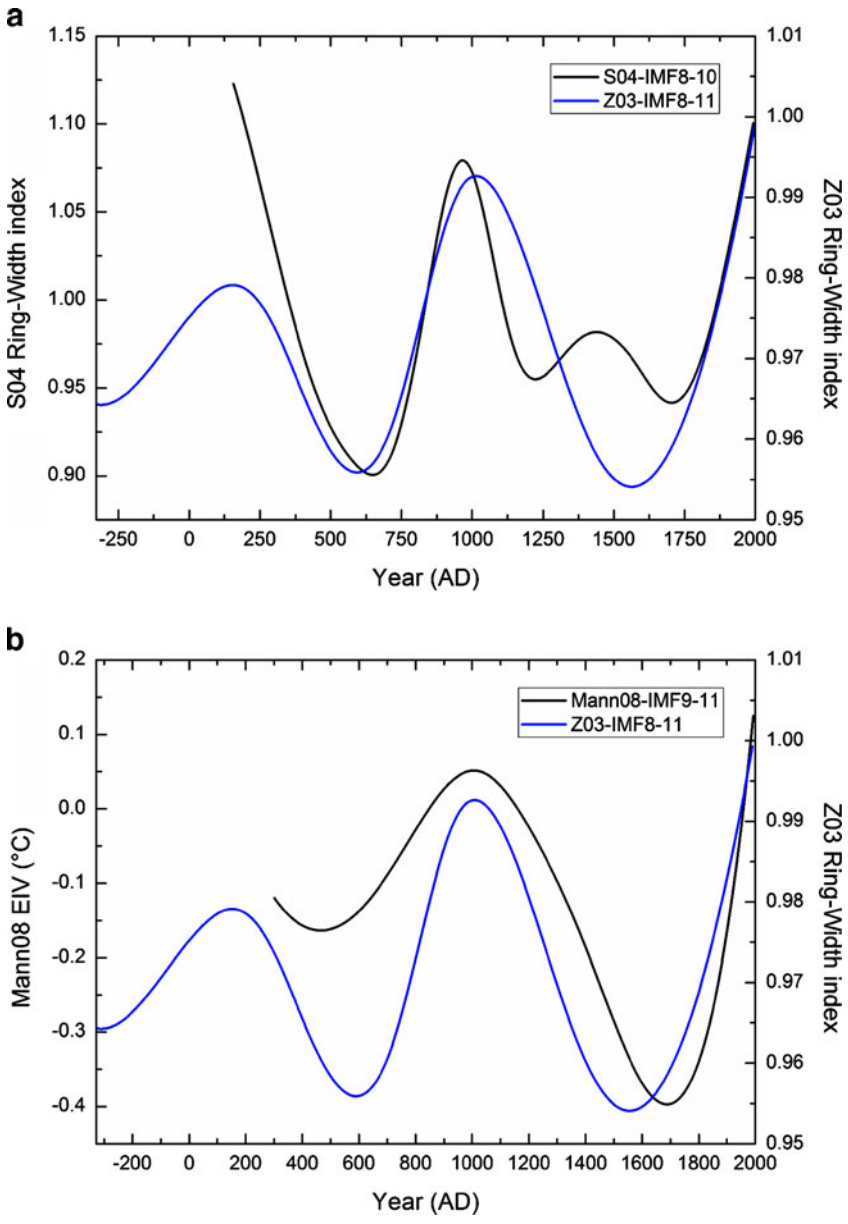

Fig. 8 **a** Comparison of the sum of the 8th to 10th IMFs of S04 with the sum of the 8th to 11th IMFs of Z03. **b** Comparison of centennial-scale changes of the Z03 chronology with the Northern Hemisphere temperature curve reported by Mann et al. (2008) for the period AD 900–2000

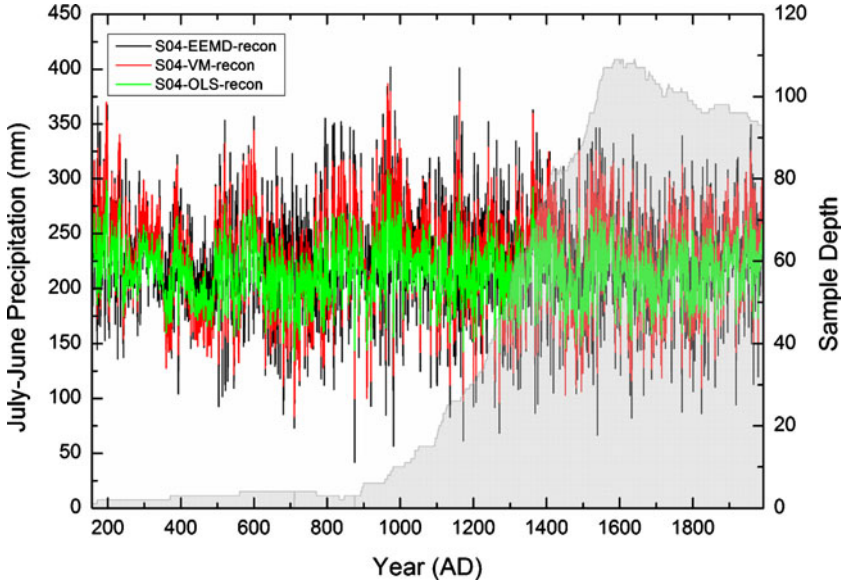

Fig. 9 Comparison of the three July–June precipitation reconstructions (EEMD, OLS, and VM) over the whole reconstruction period (AD 157–1993). The sample depths show the number of available samples

instrumental data series. It is worth noting that the summed components of the eight to 10th IMFs (i.e., the low-frequency signal) of S04 and of the eight to 11th IMFs of Z03 show very consistent low-frequency variations (Fig. 8a). Figure 8b also shows that the centennial-scale variability in the Z03 chronology and in the Northern Hemisphere temperature anomaly reported by Mann et al. (2008), respectively, are linearly and significantly correlated (r=0.90, p=0.10) during the period AD 900–2000. More comparisons between the low-frequency Northern Hemisphere temperature data and the two chronologies are presented in Fig. S1.

The above comparisons show that the tree-ring widths of the Dulan chronology were wider during the Medieval Climate Anomaly, narrower during the Little Ice Age, and wider again during the twentieth century, thereby demonstrating that the Dulan tree-ring chronology is able to capture low-frequency climate variations (Liu et al. 2009).

A comparison of the EEMD reconstruction with the conventional linear reconstructions (OLS and VM) in Fig. 9 shows that the three reconstructions yielded similar overall trends but that the standard deviations in the different time–frequency domains were significantly different. To test which one of the reconstruction techniques preserved the most accurate low-frequency information, we compared the standard deviation and mean values of the three reconstructions with instrumental data over the period AD 1955–1993. The mean and standard deviation of the precipitation reconstruction using the OLS method were 230.2 and 23.1 mm, respectively, while the mean and standard deviation of the reconstruction obtained using the direct variance matching method were 250.5 and 40.4 mm, respectively. As expected, the standard deviation of the EEMD method was the highest (up to 51.9 mm, mean 243.8 mm). The "target" standard deviation of the instrumental data is up to 51.7 mm, with a mean of 236.9 mm. The results for S04 show that the EEMD approach yielded the best results (Fig. 10). Further details on the statistical validation of the reconstruction, as well as skill assessments and uncertainty estimates, are provided in Table S4.

Because the sample depth (number of samples per year) was small before AD 1200 and the regional representation was low, we focus our discussion on the period after AD 1200. Figure 11 shows a comparison between the reconstruction of the last two components and the OLS reconstruction for S04. It can be seen that the EEMD precipitation reconstruction has a much higher low-frequency variation. Periods with greatest precipitation occurred during AD 1350–1425, 1520–1580, and 1730–1785; the annual

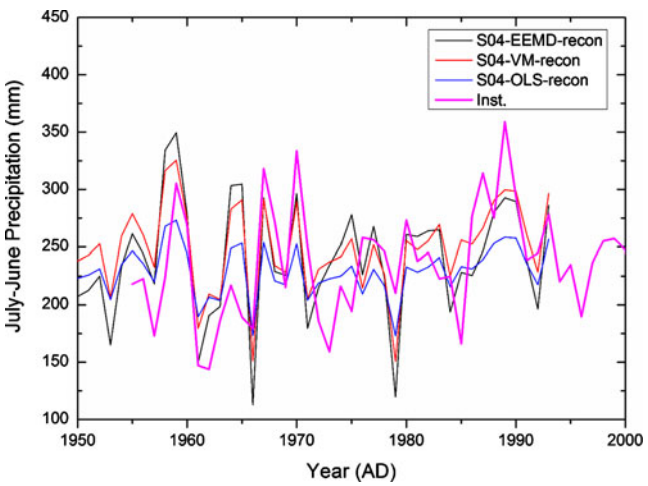

Fig. 10 Comparison of the three SO4 July–June precipitation reconstructions (EEMD, VM, and OLS) with instrumental data over the period AD1955–1993

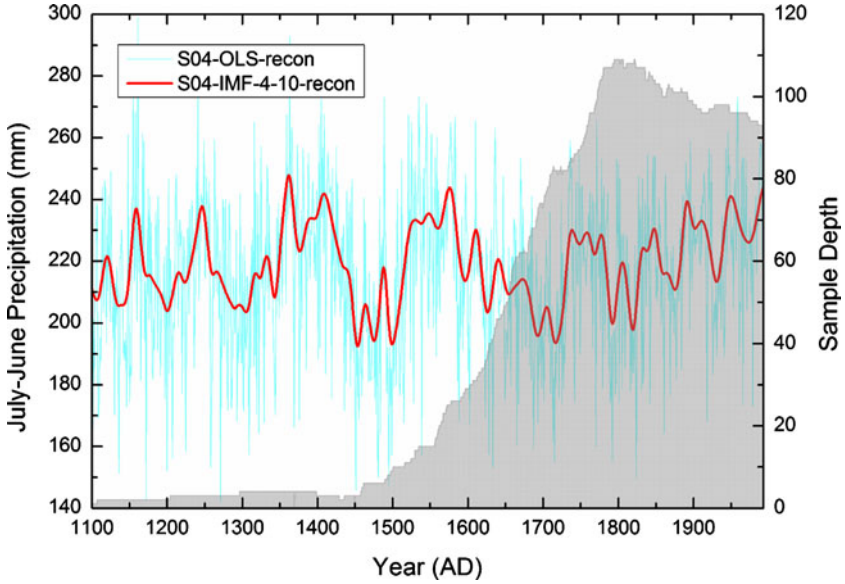

Fig. 11 Comparison of the summed 4th to 10th IMFs reconstructed by linear fitting (OLS) for the period AD 1100–1993. The sample depth shows the number of available samples

precipitation has been more stable and at a relatively high level since 1850; periods of low precipitation occurred during AD 1270–1330, 1450–1480, and 1620–1700.

The correlation coefficient between the two tree-ring chronologies was only 0.17 (p=0.31) in the period AD 1955–1993. According to the traditional linear fitting method applied to the instrumental data segment, the two tree-ring chronologies represent climatic conditions in different months. However, it can be seen that the two reconstructed annual precipitation series, based on the two chronologies, almost overlap after AD 1200 in Fig. 12. Because of the different variability of the two chronologies during the calibration period, the original authors of the Z03 reconstruction considered that Z03 was mainly sensitive to spring (May–June) precipitation variations (Zhang et al. 2003), while the authors of the original S04 reconstruction considered that S04 was sensitive to annual (July–June) precipitation variations (Sheppard et al. 2004). This indicates that care is needed when assessing which season a single tree-ring record is used to reconstruct, especially if the calibration period is short. A sound understanding of the physiological response of the tree to the changing climate should be seen as the key factor in deciding which season to reconstruct and weigh more heavily in the calibration statistics. Therefore, the EEMD method might help to solve the problems related to the heterogeneity of tree-ring chronologies during the calibration period.

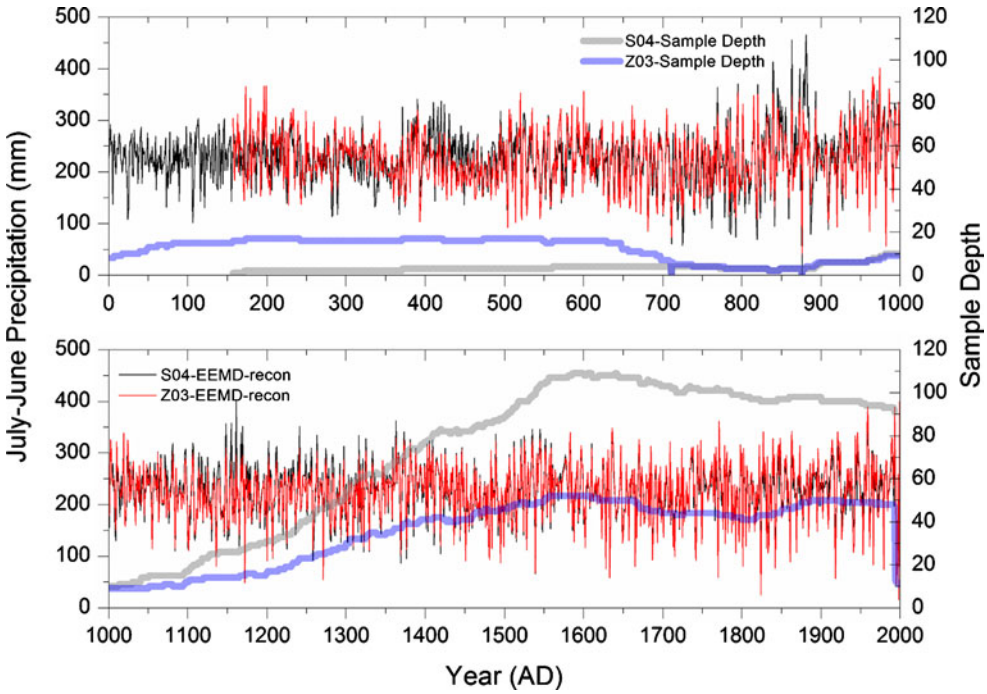

Fig. 12 Comparison of the S04 and Z03 EEMD July–June precipitation reconstructions (AD 157–1993 and 328 BC–AD 2000). The sample depths show the number of available samples

4 Conclusions

Paleoclimate reconstruction methods rarely consider the non-stationary and non-linear features of instrumental and proxy data. Here, these features in data from a case study on the Qinghai–Tibetan Plateau were analyzed using the EEMD method. Based on the different time–frequency domains identified, the Dulan precipitation series over the past millennium was reconstructed using two tree-ring width STD chronologies. Compared with the conventional reconstruction results, the EEMD method better extracts the low-frequency signals in the tree-ring chronology and better reconstructs the low-frequency variability in the Dulan climate. Furthermore, the EEMD method can also be used as an effective approach to reducing problems associated with the different time scales of variability in tree-ring chronologies relative to those in accompanying meteorological data during a calibration period. We believe that the EEMD method could be applied to many existing records to extract potentially valuable climate information.

Acknowledgements The authors thank two anonymous reviewers for their thoughtful and constructive comments. This paper also benefited from revisions by the editor Hartmut Graßl. The study was jointly funded by CAS Strategic Priority Research Program Grant (No. XDA05080801), Chinese Academy of Sciences (CAS) 100 Talents Project (29082762), and NSFC (Grant Nos. 41071130 and 40871091). Feng Shi was supported by West Light Program for Talent Cultivation of Chinese Academy of Sciences. Bao Yang gratefully acknowledges the support of K.C. Wong Education Foundation. Hong Kong. LvG was supported by Swiss NSF (PBBEP2-126056).

References

Briffa KR, Jones PD, Bartholin TS, Eckstein D, Schweingruber FH, Karlen W, Zetterberg P, Eronen M (1992) Fennoscandian summers from AD 500: temperature changes on short and long timescales. Clim Dyn 7(3):111–119

Briffa KR, Shishov VV, Melvin TM, Vaganov EA, Grudd H, Hantemirov RM, Eronen M, Naurzbaev MM (2008) Trends in recent temperature and radial tree growth spanning 2000 years across northwest Eurasia. Philos Trans Royal Soc B: Biol Sci 363(1501):2269–2282

Brohan P, Kennedy J, Harris I, Tett S, Jones P (2006) Uncertainty estimates in regional and global observed temperature changes: a new dataset from 1850. J Geophys Res 111:D12106. doi:10.1029/2005JD006548

Cook ER, Anchukaitis KJ, Buckley BM, D'Arrigo RD, Jacoby GC, Wright WE (2010) Asian monsoon failure and megadrought during the last millennium. Science 328(5977):486–489

Esper J, Cook E, Schweingruber F (2002) Low-frequency signals in long tree-ring chronologies for reconstructing past temperature variability. Science 295(5563):2250–2253

Feng S, Tang M, Wang D (1998) New evidence for the Qinghai–Xizang (Tibet) Plateau as a pilot region of climatic fluctuation in China. Chin Sci Bull 43(20):1745–1749

Glickman TS, Zenk W (2000) Glossary of meteorology. American Meteorological Society, Boston

Gou X, Yang M, Peng J, Zhang Y, Chen T, Hou Z (2006) Maximum temperature reconstruction for Animaqing Mountains over past 830 years based on tree ring records. Quat Sci 26(6):991–998 (In Chinese)

Huang NE, Wu ZH (2008) A review on Hilbert–Huang transform: method and its applications to geophysical studies. Rev Geophys 46:RG2006. doi:10.1029/2007RG000228

Huang N, Shen Z, Long S, Wu M, Shih H, Zheng Q, Yen N, Tung C, Liu H (1998) The empirical mode decomposition and the Hilbert spectrum for nonlinear and non-stationary time series analysis. Proc: Math, Phys Eng Sci 454(1971):903–995

Jones PD, Briffa KR, Barnett TP, Tett SFB (1998) High-resolution palaeoclimatic records for the last millennium: interpretation, integration and comparison with General Circulation Model control-run temperatures. Holocene 8(4):455–471

Kang XC, Graumlich L, Sheppard P (1997) A 1835-year tree-ring chronology and its preliminary analyses in Dulan region, Qinghai. Chin Sci Bull 42(13):1122–1124 (In Chinese)

Lee T, Ouarda T (2011) Prediction of climate nonstationary oscillation processes with empirical mode decomposition. J Geophys Res-Atmos 116:D06107. doi:10.1029/2010jd015142

Lee TCK, Zwiers FW, Tsao M (2008) Evaluation of proxy-based millennial reconstruction methods. Clim Dyn 31(2–3):263–281

Li QX, Dong WJ, Li W, Gao XR, Jones P, Kennedy J, Parker D (2010) Assessment of the uncertainties in temperature change in China during the last century. Chin Sci Bull 55(19):1974–1982

Liu X, Chen B (2000) Climatic warming in the Tibetan Plateau during recent decades. Int J Climatol 20(14):1729–1742

Liu X, Qin D, Shao X, Chen T, Ren J (2005) Temperature variations recovered from tree-rings in the middle Qilian Mountain over the last millennium. Sci China Ser D: Earth Sci 48(4):521–529

Liu Y, An Z, Ma H, Cai Q, Liu Z, Kutzbach J, Shi J, Song H, Sun J, Yi L (2006) Precipitation variation in the northeastern Tibetan Plateau recorded by the tree rings since 850 AD and its relevance to the Northern Hemisphere temperature. Sci China Ser D: Earth Sci 49(4):408–420

Liu Y, An Z, Linderholm H, Chen D, Song H, Cai Q, Sun J, Tian H (2009) Annual temperatures during the last 2485 years in the mid-eastern Tibetan Plateau inferred from tree rings. Sci China Ser D: Earth Sci 52(3):348–359

Mann ME, Zhang ZH, Hughes MK, Bradley RS, Miller SK, Rutherford S, Ni FB (2008) Proxy-based reconstructions of hemispheric and global surface temperature variations over the past two millennia. Proc Natl Acad Sci U S A 105(36):13252–13257

Melvin T, Briffa K (2008) A signal-free approach to dendroclimatic standardisation. Dendrochronologia 26(2):71–86

Moberg A, Sonechkin DM, Holmgren K, Datsenko NM, Karlen W (2005) Highly variable Northern Hemisphere temperatures reconstructed from low- and high-resolution proxy data. Nature 433 (7026):613–617

Qian C, Wu Z, Fu C, Zhou T (2010) On multi-timescale variability of temperature in China in modulated annual cycle reference frame. Adv Atmos Sci 27(5):1169–1182

Shao X, Huang L, Liu H, Liang E, Fang X, Wang L (2005) Reconstruction of precipitation variation from tree rings in recent 1000 years in Delingha, Qinghai. Sci China (Ser D) 48(7):939–949

Shao X, Wang S, Zhu H, Xu Y, Liang E, Yin Z, Xu X, Xiao Y (2009) A 3585-year ring-width dating chronology of Qilian juniper from the northeastern Qinghai–Tibetan Plateau. IAWA J 30(4):379–394

Sheppard P, Tarasov P, Graumlich L, Heussner K, Wagner M, Sterle H, Thompson L (2004) Annual precipitation since 515 BC reconstructed from living and fossil juniper growth of northeastern Qinghai Province, China. Clim Dyn 23(7):869–881

Tang G, Ding Y, Wang S, Ren G, Liu H, Zhang L (2009) Comparative analysis of the time series of surface air temperature over China for the last 100 years. Adv Clim Chang Res 5(2):71–78

Torrence C, Compo GP (1998) A practical guide to wavelet analysis. Bull Am Meteorol Soc 79(1):61–78

Trenberth KE (1984) Some effects of finite sample size and persistence on meteorological statistics. part I: Autocorrelations. Mon Wea Rev 112:2359–2368

Webster P, Tomas R (1998) Monsoons—processes, predictability, and the prospects for prediction. J Geophys Res 103(C7):14451–14510

Wu Z, Schneider E, Kirtman B, Sarachik E, Huang N, Tucker C (2008) The modulated annual cycle: an alternative reference frame for climate anomalies. Clim Dyn 31(7):823–841

Wu Z, Huang N, Chen X (2009) The multi-dimensional ensemble empirical mode decomposition method. Adv Adapt Data Anal 1 (3):339–372

Wu Z, Huang N, Wallace J, Smoliak B, Chen X (2011) On the time-varying trend in global-mean surface temperature. Clim Dyn 37(3):759–773

Yang B, Kang XC, Brauning A, Liu J, Qin C, Liu JJ (2010) A 622-year regional temperature history of southeast Tibet derived from tree rings. Holocene 20(2):181–190

Yang B, Qin C, Bräuning A, Burchardt I, Liu J (2011) Rainfall history for the Hexi Corridor in the arid northwest China during the past 620 years derived from tree rings. Int J Climatol 31(8):1166–1176

Yang B, Sonechkin DM, Datsenko NM, Ivashchenko NN, Liu J, Qin C (2012a) Eigen analysis of tree-ring records: part 2, posing the eigen problem. Theor Appl Climatol. doi:10.1007/s00704-011-0468-y

Yang B, Sonechkin DM, Datsenko NM, Ivashchenko NN, Liu J, Qin C (2012b) The eigen analysis of tree-ring records: part 3, taking heteroscedasticity and sampling effects into consideration. Theor Appl Climatol. doi:10.1007/s00704-011-0498-5

Zhang Q, Qiu H (2007) A millennium-long tree-ring chronology of *Sabina przewalskii* on northeastern Qinghai–Tibetan Plateau. Dendrochronologia 24(2–3):91–95

Zhang Q, Cheng G, Yao T, Kang X, Huang J (2003) A 2,326-year tree-ring record of climate variability on the northeastern Qinghai–Tibetan Plateau. Geophys Res Lett 30(14):1739–1742

Zhang Y, Gou X, Chen F, Tian Q, Yang M, Peng J, Fang K (2009) A 1232-year tree-ring record of climate variability in the Qilian Mountains, northwestern China. IAWA J 30(4):407–420

Zhu H, Zheng Y, Shao X, Liu X, Xu Y, Liang E (2008) Millennial temperature reconstruction based on tree-ring widths of Qilian juniper from Wulan, Qinghai Province, China. Chin Sci Bull 53 (24):3914–3920